

# On the anomalous large-scale flows in the Universe

Davor Palle

*Zavod za teorijsku fiziku, Institut Rugjer Bošković*

*Bijenička cesta 54, 10001 Zagreb, Croatia*

(Dated: February 10, 2009)

## Abstract

Recent combined analyses of the CMB and galaxy cluster data reveal unexpectedly large and anisotropic peculiar velocity fields at large scales. We study cosmic models with included vorticity, acceleration and total angular momentum of the Universe in order to understand the phenomenon. The Zeljdovič model is used to mimic the low redshift evolution of the angular momentum. Solving coupled evolution equations of the second kind for density-contrast in corrected Ellis-Bruni covariant and gauge-invariant formalism one can properly normalize and evaluate integrated Sachs-Wolfe effect and peculiar velocity field. The theoretical results compared to the observations favour a much larger matter content of the Universe than that of the concordance model. Large-scale flows appear anisotropic with dominant components placed in the plane perpendicular to the axis of vorticity (rotation). The integrated Sachs-Wolfe term has negative contribution to the CMB fluctuations for the negative cosmological constant and it can explain the observed small power of the CMB TT spectrum at large scales. The rate of the expansion of the Universe can be substantially affected by the angular momentum if its magnitude is large enough.

PACS numbers: 98.80.Es; 12.10.Dm; 04.60.-m

## I. INTRODUCTION AND MOTIVATION

The phenomenology of particle physics, cosmology and astroparticle physics should be understood with the unique physical principles. Heavy Majorana neutrinos within the non-singular and causal SU(3) electroweak-strong unification [1] represent the main building block of the Universe as a cold dark matter (DM) particles. They are cosmologically stable  $\tau_{N_i} \gg \tau_U$  with large annihilation cross sections [2]. The H.E.S.S. source J1745-290 [3] in the center of our galaxy, WMAP haze [4] and EGRET excess of diffuse photon background are possible indications of the heavy DM particle annihilations.

Light Majorana neutrinos trigger vorticity of the Universe [5, 6] through the spin-torsion connection in the Einstein-Cartan cosmology at early times of the evolution. The formation of large-scale structures in the form of galaxies and clusters, as well as, the present anisotropy of spacetime, indicate the existence of nonvanishing total angular momentum of the Universe.

The current measurements of the CMB by WMAP, the large catalogues of SDSS, the new cluster and the peculiar velocity catalogues motivate us to undertake considerations to explain features that are not expected in the concordance  $\Lambda$ CDM model.

In the next chapter we derive the evolution equations of density-contrast for models with expansion, vorticity, acceleration and angular momentum within the corrected Ellis-Bruni formalism. A comparison is made with the standard formulas of isotropic and homogeneous spacetime. One can then evaluate integrated Sachs-Wolfe effect and RMS peculiar velocity field for any model.

The last chapter is devoted for discussions, conclusions and suggestions for future work. Appendices contain detailed framework for Einstein-Cartan cosmology with field equations, propagation equations and a comparison of the corrected and standard Ellis-Bruni fluid flow approach for the density-contrast evolution.

## II. EVOLUTION EQUATIONS

Our interest is the evolution of the Universe during the matter dominated epoch. The standard lore for the evolution of the density contrast, peculiar acceleration and peculiar velocity field gives the following equations [7, 8, 9]:

$$\delta(a, \vec{k}) \equiv \delta(a)\delta_{\vec{k}}, \quad \delta(\vec{x}) = \int d^3k e^{i\vec{k}\cdot\vec{x}}\delta_{\vec{k}},$$

$$\vec{v}_{\vec{k}} = \frac{i\vec{k}}{k^2} a \dot{a} \delta_{\vec{k}} \frac{d\delta(a)}{da}, \quad a = R(t)/R_0 = 1/(1+z). \quad (1)$$

The root mean square (RMS) values of the mass-density contrast and the peculiar velocity field at a certain scale  $R$  and the redshift  $z$  using Gaussian window functions [7, 8, 9] are defined as:

$$(\delta M/M)_{RMS}^2(a, R) \equiv \langle (\delta M/M)^2 \rangle(a, R) = NV_W^{-2} \int d^3k W^2(\vec{k}, R) \delta^2(a) |\delta_{\vec{k}}|^2, \quad (2)$$

$$v_{RMS}^2(a, R) \equiv \langle v^2 \rangle(a, R) = NV_W^{-2} \int d^3k W^2(\vec{k}, R) \frac{1}{k^2} (a \dot{a} \frac{d\delta(a)}{da})^2 |\delta_{\vec{k}}|^2, \quad (3)$$

$$V_W = \frac{4\pi}{3} R^3, \quad W(\vec{k}, R) = (2\pi)^{3/2} R^3 e^{-\frac{1}{2}R^2 \vec{k}^2}.$$

The aim is to study cosmological models with vorticity, acceleration and nonvanishing total angular momentum through torsion effects. We use the standard CDM power spectrum  $P(k) = |\delta_{\vec{k}}|^2$  defined in [8].

The growth function  $\delta(a)$  must be studied carefully. Our choice of covariant spacelike vectors within a fluid flow formalism differs from that of Ellis and Bruni [10]:

$$\mathcal{D}_\mu \equiv R^2(t) \rho^{-1} h_\mu^\nu \tilde{\nabla}_\nu \rho, \quad (4)$$

$$\mathcal{L}_\mu \equiv R^2(t) h_\mu^\nu \tilde{\nabla}_\nu \Theta.$$

These vectors fulfil the Stewart-Walker lemma [11] and their evolution equations result in a correct solution for a density-contrast formed from their scalar invariants. This is not the case for the standard Ellis-Bruni covariant vectors.

The detailed derivation of the equations one can find in the Appendix A while a comparison between two fluid-flow approaches is in the Appendix B.

The resulting second order coupled equations in our corrected scheme are given by (matter dominated regime):

$$\begin{aligned}
& \ddot{\mathcal{D}}_\mu - \frac{1}{3}\dot{\Theta}\mathcal{D}_\mu - \frac{1}{3}\Theta\dot{\mathcal{D}}_\mu + a_\mu a^\nu \mathcal{D}_\nu + u_\mu \dot{a}^\nu \mathcal{D}_\nu + u_\mu a^\nu \dot{\mathcal{D}}_\nu \\
& - \left(\frac{1}{3}\Theta\delta_\mu^\lambda + u_\mu a^\lambda + \tilde{\omega}_{\cdot\mu}^\lambda + \sigma_{\cdot\mu}^\lambda\right) \left(\frac{1}{3}\Theta\mathcal{D}_\lambda - u_\lambda a^\nu \mathcal{D}_\nu - \dot{\mathcal{D}}_\lambda - \mathcal{D}_\rho(\sigma_{\cdot\lambda}^\rho + \tilde{\omega}_{\cdot\lambda}^\rho) + \Theta R^2 a_\lambda\right) \\
& - 2a_\mu R^2 \dot{\Theta} - R^2({}^{(3)}\tilde{\nabla}_\mu \mathcal{N}) - \frac{1}{2}\kappa\rho\mathcal{D}_\mu + \dot{\mathcal{D}}_\lambda(\sigma_{\cdot\mu}^\lambda + \tilde{\omega}_{\cdot\mu}^\lambda) \\
& + \mathcal{D}_\lambda(\dot{\sigma}_{\cdot\mu}^\lambda + \dot{\tilde{\omega}}_{\cdot\mu}^\lambda) - \frac{2}{3}R^2\Theta^2 a_\mu - \Theta R^2 \dot{a}_\mu = 0, \quad (5)
\end{aligned}$$

$$\mathcal{N} = 2\sigma^2 - 2\tilde{\omega}^2 - \tilde{\nabla}_\mu a^\mu.$$

We use the Zeljdovič model to describe the evolution of the total angular momentum of the Universe at small redshifts [9] assuming the surplus of right-handed over left-handed galaxies and clusters [6, 12]

$$\begin{aligned}
\vec{L}(t) & \propto a^2 \dot{a} \bar{\rho} \int_{V_L} d^3q (\vec{q} - \vec{\bar{q}}) \times [\vec{\nabla}\Phi_0(q) - \vec{\nabla}\Phi_0(\bar{q})], \\
\vec{L}(Universe) & \propto [n(right) - n(left)] \vec{L}(t), \\
Q = torsion & \propto L(Universe) \Rightarrow Q(a) = Q_0 a^{-3/2} \text{ for } z = a^{-1} - 1 < z_{cr} = 4, \quad (6) \\
& \text{where } z_{cr} = 4 \text{ is put arbitrarily, otherwise } Q(z > z_{cr}) = 0.
\end{aligned}$$

The Einstein-Cartan equations remain unaltered with respect to the functional form of the time dependence of torsion (see Appendix A).

We have to factorize density-contrast on the space and time dependent parts. One can achieve this goal transforming the evolution equations for covariant vectors to the local Lorentzian frame by tetrads:

$$\mathcal{D}_a = v_a^\mu \mathcal{D}_\mu, \quad g^{\mu\nu} = v_a^\mu v_b^\nu \eta^{ab}, \quad \delta = (-\mathcal{D}_a \mathcal{D}^a)^{1/2},$$

$$\eta^{ab} = \text{diag}(+1, -1, -1, -1), \quad \mu, \nu = 0, 1, 2, 3, \quad a, b = \hat{0}, \hat{1}, \hat{2}, \hat{3}.$$

In the Appendix A one can find evaluated coefficients for the following spacetime metric:

$$\begin{aligned}
ds^2 & = dt^2 - R^2(t)[dx^2 + (1 - \lambda^2(t))e^{2mx} dy^2] - R^2(t)dz^2 - 2R(t)\lambda(t)e^{mx} dydt, \quad (7) \\
& m = \text{const.}
\end{aligned}$$

It is easy to verify that in the Friedmann limit one recovers the standard form of the density-contrast [13] (see Appendix A):

$$\begin{aligned}\delta(a) &= \frac{H(a)}{H_0} \int_0^a da a^{-3} \left[ \frac{H_0}{H(a)} \right]^3, \\ H(a) &= H_0 (\Omega_m a^{-3} + \Omega_\Lambda)^{1/2}.\end{aligned}\tag{8}$$

One can evaluate properly normalized peculiar velocities and integrated Sachs-Wolfe effect for various cosmological models [13]:

$$\begin{aligned}a_{lm}^{ISW} &= 12\pi i^l \int d^3k Y_l^{m*}(\hat{k}) \delta_{\vec{k}} \left( \frac{H_0}{k} \right)^2 \int da j_l(kr) \chi^{ISW}, \\ \chi^{ISW} &= -\Omega_m \frac{d}{da} (\delta(a)/a), \quad r = \int_a^1 da a^{-2} H^{-1}(a), \quad \delta(a=1) = 1.\end{aligned}\tag{9}$$

### III. RESULTS AND DISCUSSION

Supplied with all the necessary equations we can evaluate properly normalized peculiar velocities and integrated Sachs-Wolfe effect. We use the same normalization for all cosmological models:

$$(\delta M/M)_{RMS}(a=1, R=10h^{-1}Mpc) = 1.$$

Let us fix relevant parameters of the models in Table I (unit  $H_0 = 1$  is used for parameters  $m$ ,  $\lambda_0$  and  $Q_0$ ; EdS=Einstein-de Sitter, EC=Einstein-Cartan,  $\Lambda$ CDM=concordance model,  $\Omega_\Lambda = 1 - \Omega_m$ ,  $\lambda = \lambda_0 R^{-1}$ ,  $Q = Q_0 R^{-3/2}$ ,  $R_0 = H_0^{-1}$  ).

The formation of small-scale structures and the age of the Universe can be explained with a larger mass-density and smaller Hubble constant (see Table II). This statement is valid if we assume that the total angular momentum of the Universe at low redshifts, acting through torsion terms, is much smaller than mass-density terms. The evolution with large torsion terms must contain feedback from matter to the background geometry, changing substantially its expansion and vorticity. It is possible to utilize this approach within N-body simulations. Thus, we limit numerical evaluations in this paper to small torsion contributions.

	$\Omega_m$	h	m	$\lambda_0$	$Q_0$
$\Lambda$ CDM	0.3	0.7	0	0	0
EdS	1	0.5	0	0	0
EC1	2	0.4	0.03	0.067	-0.2
EC2	2	0.4	0	0	0
EC3	2	0.4	0.3	0.67	0

TABLE I: Model parameters

	$\Lambda$ CDM	EdS	EC1	EC2
$\tau_U$ (Gyr)	13.77	13.33	13.14	13.09

TABLE II: Age of the Universe

From Tables III-VI it is clear that only models with large mass-density can enhance large-scale peculiar velocities observed in the analyses with combined cluster and WMAP data [14, 15]. Rather small amounts of vorticity, acceleration or torsion do not essentially influence RMS velocities. However, components of a density-contrast  $\mathcal{D}_i, i = 1, 2, 3$  are not equal. We assume the standard scaling of the vorticity [7]:  $\lambda(a) = \lambda_0 a^{-1} \Rightarrow \omega \propto a^{-2}$  (see Appendix A for definitions).

The density-contrasts normalized at zero-redshift do not depend on the initial cosmic scale factor, but a difference between components does depend. One can estimate the resulting angle between the axis of vorticity (z-axis) and the anisotropic bulk velocity. The angle depends on the initial redshift and the magnitude of the vorticity ( $\omega(t) = \frac{1}{2}m\lambda(t)R(t)^{-1}$ ):

$$a(\text{initial}) = 10^{-2}, a(\text{final}) = 1, \text{ model} = \text{EC1}, \frac{\omega_0}{H_0} = \frac{1}{2}m\lambda_0 = 10^{-3}$$

$$\Rightarrow \angle(\hat{n}(\text{flow}), \hat{n}(\text{axis})) = \text{arctg} \frac{(\mathcal{D}_1^2 + \mathcal{D}_2^2)^{1/2}}{|\mathcal{D}_3|} = 55.3^\circ,$$

$$a(\text{initial}) = 10^{-2}, a(\text{final}) = 1, \text{ model} = \text{EC1}, \text{ but } m = 0.15 : \angle(\hat{n}(\text{flow}), \hat{n}(\text{axis})) = 57.25^\circ,$$

$$a(\text{initial}) = 10^{-3}, a(\text{final}) = 1, \text{ model} = \text{EC1} : \angle(\hat{n}(\text{flow}), \hat{n}(\text{axis})) = 72.3^\circ.$$

Since the metric describes rotation around z-axis, the dominant components of over(under)densities, the peculiar accelerations and the velocities are placed in the plain

$z \setminus R(\text{Mpc})$	50	187.5	325	462.5	600
0	511.67	184.73	111.75	79.95	62.21
0.25	515.49	186.11	112.58	80.55	62.67
1	467.16	168.66	102.03	73.00	56.80

TABLE III:  $v_{rms}(km/s)$  for the  $\Lambda$ CDM model

$z \setminus R(\text{Mpc})$	50	187.5	325	462.5	600
0	766.27	245.82	145.55	103.27	80.00
0.25	685.38	218.87	130.18	92.37	71.56
1	541.84	173.82	102.92	73.03	56.57

TABLE IV:  $v_{rms}(km/s)$  for the EdS model

$z \setminus R(\text{Mpc})$	50	187.5	325	462.5	600
0	1090.94	335.81	197.54	139.83	108.19
0.25	901.75	277.58	163.28	115.58	89.42
1	678.04	208.71	122.78	86.91	67.24

TABLE V:  $v_{rms}(km/s)$  for the EC1 model

$z \setminus R(\text{Mpc})$	50	187.5	325	462.5	600
0	1091.69	336.04	197.68	139.92	108.26
0.25	902.28	277.74	163.38	115.65	89.48
1	678.45	208.84	122.85	86.96	67.28

TABLE VI:  $v_{rms}(km/s)$  for the EC2 model

perpendicular to the axis of rotation (vorticity). We estimate the angle between the measured directions of the axis of vorticity [16] and the large-scale flows [15]:

$$\begin{aligned} \hat{n}(flow) &= (l = 287^\circ, b = 8^\circ), \quad \hat{n}(axis) = (l = 260^\circ, b = 60^\circ) \\ &\Rightarrow \angle(\hat{n}(flow), \hat{n}(axis)) = 53^\circ. \end{aligned}$$

The reader can compare and visualize density contrasts and their derivatives for two crucial models ( $\Lambda$ CDM and EC) in Figs. 1 and 2.

The integrated Sachs-Wolfe effect is negative for large mass-density models (EC) with

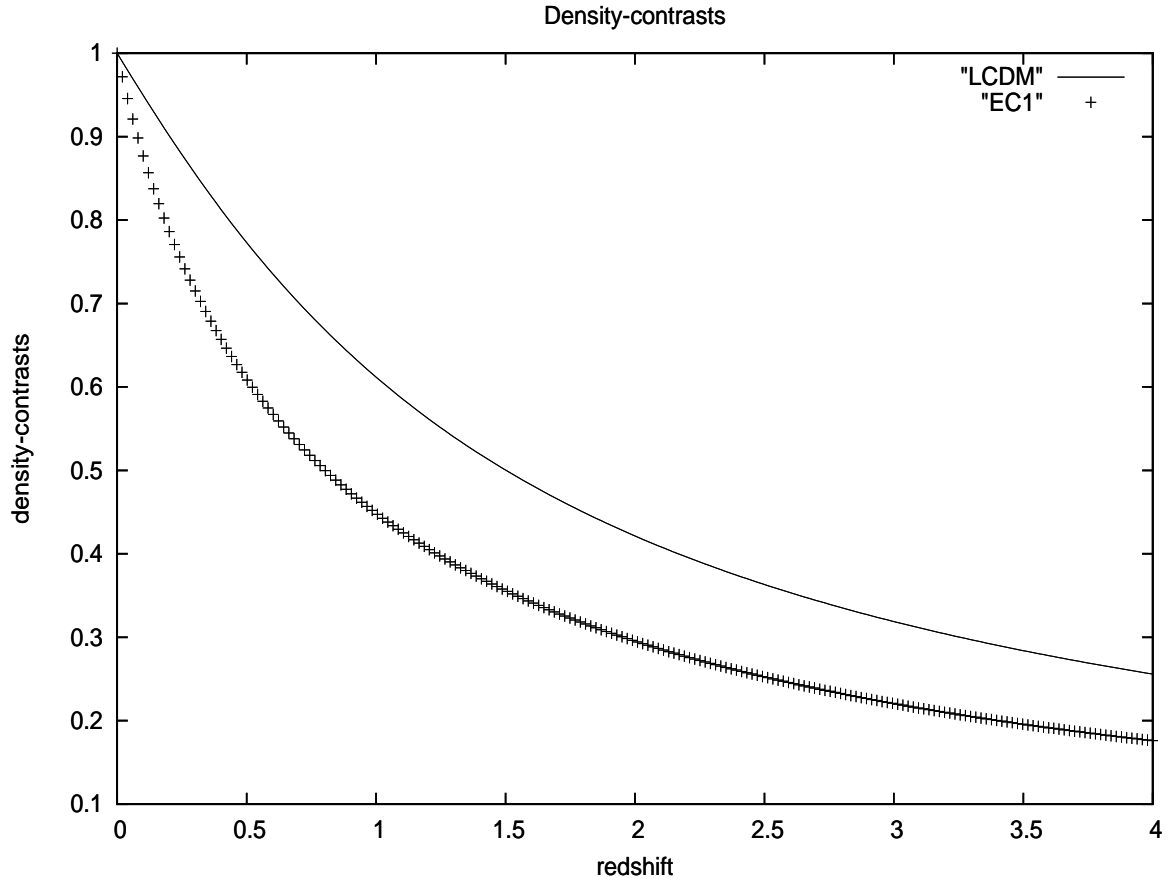


FIG. 1: Density-contrasts for the  $\Lambda$ CDM and EC1 models.

negative cosmological constant, while it is positive for  $\Lambda$ CDM, as can be seen in Fig. 3. The negative contribution can explain the small large-scale power of the CMB TT spectrum [17].

It seems that the introduction of rotational degrees of freedom (torsion, spin, vorticity, angular momentum) is inevitable in order to understand and fit all observational data. Two scenarios emerge as viable resolutions: small Hubble constant with small amount of the total angular momentum of the Universe at present or possibly larger Hubble constant if the total angular momentum appears much larger. Torsion terms (linear and quadratic) always give a negative contribution to the effective mass-density, as it can be seen from Einstein-Cartan field equations (see Appendix A). Considerations with large angular momentum (torsion) of the Universe must include large-scale N-body numerical simulations.

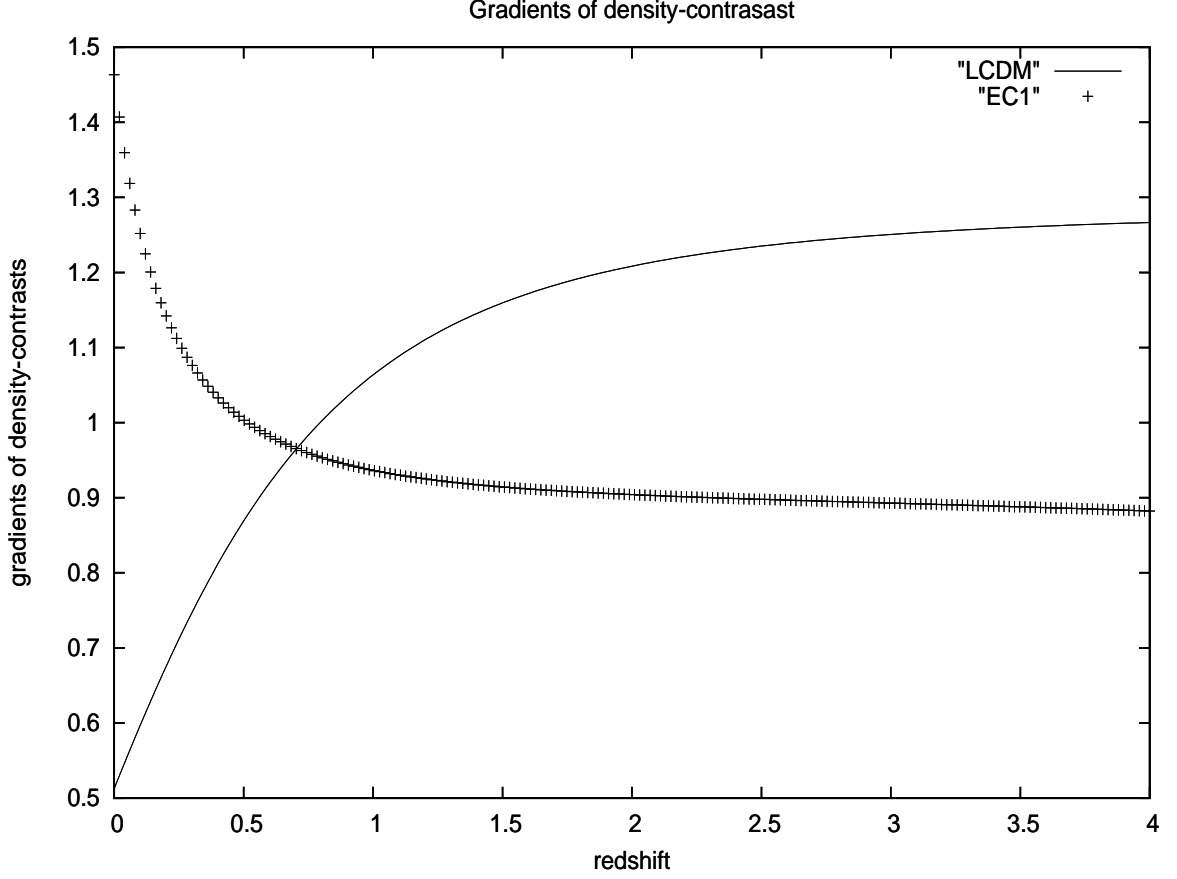


FIG. 2: Gradients of the density-contrasts  $\frac{d\delta}{da}$  for the  $\Lambda$ CDM and EC1 models.

#### IV. APPENDIX A

We provide here a complete set of conventions, identities and equations for Einstein-Cartan theory. Let us start with definitions:

$$\begin{aligned}
 g^{\mu\nu} &= v_a^\mu v_b^\nu \eta^{ab}, \quad \eta_{ab} = \text{diag}(+1, -1, -1, -1), \\
 \mu, \nu &= 0, 1, 2, 3, \quad a, b = \hat{0}, \hat{1}, \hat{2}, \hat{3}, \\
 \tilde{\Gamma}_{\beta\mu}^\alpha &= \Gamma_{\beta\mu}^\alpha + Q_{\beta\mu}^\alpha + Q_{\beta\mu}^{\cdot\cdot\alpha} + Q_{\mu\beta}^{\cdot\cdot\alpha}, \\
 \tilde{R}_{\cdot\sigma\mu\nu}^\lambda &= \partial_\mu \tilde{\Gamma}_{\sigma\nu}^\lambda - \partial_\nu \tilde{\Gamma}_{\sigma\mu}^\lambda + \tilde{\Gamma}_{\beta\mu}^\lambda \tilde{\Gamma}_{\sigma\nu}^\beta - \tilde{\Gamma}_{\beta\nu}^\lambda \tilde{\Gamma}_{\sigma\mu}^\beta.
 \end{aligned}$$

Field equations and Ricci identities look as [18]:

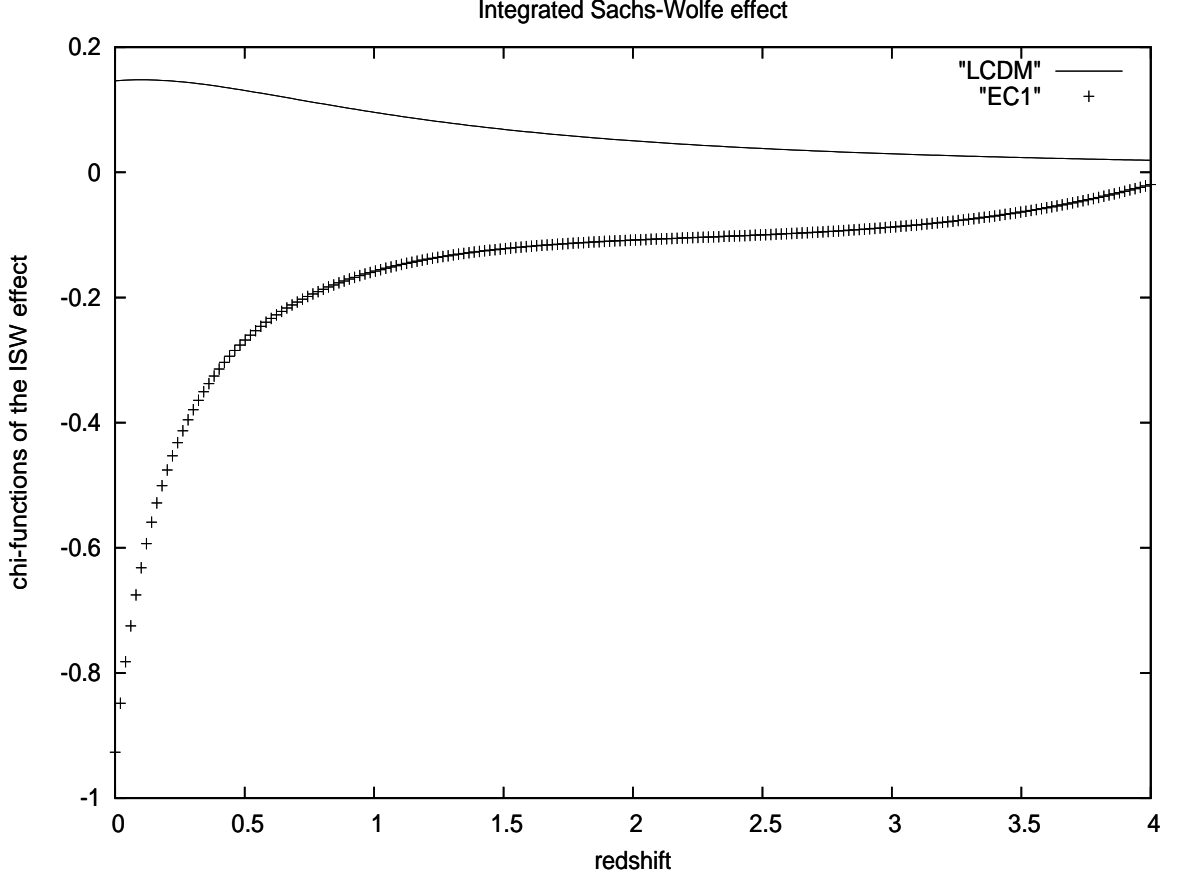


FIG. 3: Integrated Sachs-Wolfe  $\chi^{ISW}$  function for the  $\Lambda$ CDM and EC1 models.

$$\begin{aligned}
\tilde{R}_{\mu\nu} - \frac{1}{2}g_{\mu\nu}\tilde{R} &= \kappa\tilde{T}_{\mu\nu}, \quad \tilde{R}_{\mu\nu} = \tilde{R}^{\lambda}_{\cdot\mu\lambda\nu}, \quad \tilde{R} = \tilde{R}^{\mu}_{\cdot\mu}, \\
Q^{\mu}_{\cdot ab} + 2v^{\mu}_{[a}Q_{b]} &= \kappa S^{\mu}_{\cdot ab}, \quad \kappa = 8\pi G_N c^{-4}, \\
Q_a &= v^{\mu}_a Q_{\mu}, \quad Q_{\mu} = Q^{\mu}_{\cdot\mu\nu}, \quad [ab] = 1/2(ab - ba), \quad (ab) = 1/2(ab + ba) \\
(\tilde{\nabla}_{\mu}\tilde{\nabla}_{\nu} - \tilde{\nabla}_{\nu}\tilde{\nabla}_{\mu})u_{\lambda} &= -\tilde{R}^{\sigma}_{\cdot\lambda\mu\nu}u_{\sigma} - 2Q^{\sigma}_{\cdot\nu\mu}\tilde{\nabla}_{\sigma}u_{\lambda}, \\
\tilde{\nabla}_{\alpha}u_{\beta} &= \partial_{\alpha}u_{\beta} - \tilde{\Gamma}^{\nu}_{\beta\alpha}u_{\nu}.
\end{aligned}$$

Conformal or Weyl tensor  $\tilde{C}_{\sigma\lambda\mu\nu}$  is defined as:

$$\begin{aligned}
\tilde{R}_{\sigma\lambda\mu\nu} &= \frac{1}{2}(g_{\sigma\mu}\tilde{R}_{\lambda\nu} - g_{\sigma\nu}\tilde{R}_{\lambda\mu} - g_{\lambda\mu}\tilde{R}_{\sigma\nu} + g_{\lambda\nu}\tilde{R}_{\sigma\mu}) \\
&\quad - \frac{1}{6}\tilde{R}(g_{\sigma\mu}g_{\lambda\nu} - g_{\sigma\nu}g_{\lambda\mu}) + \tilde{C}_{\sigma\lambda\mu\nu}.
\end{aligned}$$

The energy-momentum tensor of the Weyssenhoff fluid is derived by Obukhov and Korkotky [19]:

$$T_{\mu\nu} = -(p - \Lambda)g_{\mu\nu} + u_\mu[u_\nu(\rho + p) + 2u^\alpha \tilde{\nabla}_\beta S_{\alpha\nu}^\beta]. \quad (10)$$

The Ehlers-decomposition of the velocity-gradient can be written as

$$\begin{aligned} \tilde{\nabla}_\mu u_\nu &= \tilde{\omega}_{\nu\mu} + \sigma_{\mu\nu} + \frac{1}{3}\Theta h_{\mu\nu} + u_\mu a_\nu, \\ u^\mu u_\mu &= 1, \quad h_{\mu\nu} = g_{\mu\nu} - u_\mu u_\nu, \quad a_\mu = u^\nu \tilde{\nabla}_\nu u_\mu, \quad \Theta = \tilde{\nabla}_\nu u^\nu, \\ \tilde{\omega}_{\mu\nu} &= h_\mu^\alpha h_\nu^\beta \tilde{\nabla}_{[\beta} u_{\alpha]}, \quad \sigma_{\mu\nu} = h_\mu^\alpha h_\nu^\beta \tilde{\nabla}_{(\alpha} u_{\beta)} - \frac{1}{3}\Theta h_{\mu\nu}. \end{aligned} \quad (11)$$

The vorticity is uniquely defined by a variational principle (see Eq. (3.11) of [19]):

$$\tilde{\omega}_{ij} = v_i^\mu (\tilde{\nabla}_\alpha v_j^\nu) u^\alpha g_{\mu\nu}, \quad i, j = \hat{1}, \hat{2}, \hat{3}. \quad (12)$$

The above two formulas for vorticity agree, but a formula for vorticity in (5.5) of [19] has a wrong sign, as well as definitions of vorticity in [20] and [21]. Eventually, this confusion caused some wrong terms in the derivation of the evolution equations in [22], as it is pointed out in [21] and later in [23].

The standard procedure leads to the evolution equations (Frenkel condition employed  $u^\mu Q_{;\mu\nu}^\kappa = 0$ ):

$$\begin{aligned} \dot{F} &\equiv u^\mu \tilde{\nabla}_\mu F, \quad \tilde{\omega}^2 = \frac{1}{2} \tilde{\omega}_{\mu\nu} \tilde{\omega}^{\mu\nu}, \quad \sigma^2 = \frac{1}{2} \sigma_{\mu\nu} \sigma^{\mu\nu}, \\ \dot{\Theta} &= \tilde{\nabla}_\mu a^\mu + 2\tilde{\omega}^2 - 2\sigma^2 - \frac{1}{3}\Theta^2 - \tilde{R}_{\sigma\nu} u^\sigma u^\nu, \\ h_\alpha^{[\nu} h_\beta^{\lambda]} \dot{\tilde{\omega}}_{\nu\lambda} &= -\frac{2}{3}\Theta \tilde{\omega}_{\alpha\beta} - 2\sigma_{[\alpha}^\gamma \tilde{\omega}_{\gamma|\beta]} - h_\alpha^{[\nu} h_\beta^{\lambda]} \tilde{\nabla}_\nu a_\lambda + h_\alpha^{[\nu} h_\beta^{\lambda]} u^\mu u^\kappa \tilde{R}_{\kappa\lambda\mu\nu}, \\ h_\nu^\alpha h_\mu^\beta \dot{\sigma}_{\alpha\beta} &= h_\nu^\alpha h_\mu^\beta \tilde{\nabla}_{(\alpha} a_{\beta)} - a_\nu a_\mu - \tilde{\omega}_{(\nu|\rho} \tilde{\omega}_{|\mu)}^\rho - \sigma_{\nu\alpha} \sigma_\mu^\alpha \\ &\quad - \frac{2}{3}\Theta \sigma_{\nu\mu} - \frac{1}{3} h_{\nu\mu} [2(\tilde{\omega}^2 - \sigma^2) + \tilde{\nabla}_\alpha a^\alpha] - E_{(\nu\mu)}, \\ E_{\alpha\beta} &= \tilde{C}_{\sigma\alpha\mu\beta} u^\sigma u^\mu. \end{aligned}$$

We use the following identity:

$${}^{(3)}\tilde{\nabla}_\mu(\dot{f}) - h_\mu^\nu({}^{(3)}\tilde{\nabla}_\nu f)^\cdot = a_\mu \dot{f} + (\tilde{\omega}_\mu^\lambda + \sigma_\mu^\lambda + \frac{1}{3}\Theta h_\mu^\lambda){}^{(3)}\tilde{\nabla}_\lambda f, \quad (13)$$

and the continuity equation in matter dominated epoch:

$$u^\mu \tilde{\nabla}_\mu \rho + \rho \tilde{\nabla}_\mu u^\mu = 0 \quad (14)$$

to derive the evolution equation for density-contrast Eq.(5).

We evaluate the coefficients of the coupled evolution equations for components in the local Lorentzian frame  $\mathcal{D}_a$  with the metric of Eq.(7) (time component  $\mathcal{D}_0$  can be set to zero because of the relation  $u^a \mathcal{D}_a = 0$ ):

$$\ddot{\mathcal{D}}_i + b_{ij} \dot{\mathcal{D}}_j + a_{ik} \mathcal{D}_k + d_i = 0, \quad i, j, k = 1, 2, 3, \quad (15)$$

$$\begin{aligned} a_{11} &= -\frac{1}{3}\dot{\lambda}^2 - \frac{1}{3}\kappa\Lambda - \frac{5}{3}Q^2 - \frac{1}{3}\kappa\rho - \frac{5}{3}\frac{\dot{R}}{R}\lambda\dot{\lambda} \\ &\quad - \frac{1}{3}\ddot{\lambda}\lambda + \frac{5}{3}\frac{m}{R}\lambda Q - \frac{2}{3}\lambda^2\frac{\dot{R}^2}{R^2} - \frac{5}{12}\left(\lambda\frac{m}{R}\right)^2 - \frac{1}{3}\frac{\ddot{R}}{R}(-3 + \lambda^2), \\ a_{12} &= \frac{1}{2}\frac{m}{R}\dot{\lambda} + \frac{1}{4}\frac{\dot{R}}{R}Q + \frac{1}{2}\lambda\frac{m}{R}\frac{\dot{R}}{R}, \quad a_{13} = 0, \\ b_{11} &= 2\frac{\dot{R}}{R}, \quad b_{12} = -2Q + \lambda\frac{m}{R}, \quad b_{13} = 0, \\ \\ a_{21} &= -\frac{1}{2}\frac{m}{R}\dot{\lambda} - \frac{1}{4}\frac{\dot{R}}{R}Q - \frac{1}{2}\lambda\frac{m}{R}\frac{\dot{R}}{R}, \\ a_{22} &= -\frac{4}{3}\dot{\lambda}^2 - \frac{1}{3}\kappa\Lambda - \frac{5}{3}Q^2 - \frac{1}{3}\kappa\rho - \frac{11}{3}\frac{\dot{R}}{R}\lambda\dot{\lambda} \\ &\quad - \frac{1}{3}\ddot{\lambda}\lambda + \frac{5}{3}\frac{m}{R}Q\lambda - \frac{5}{3}\lambda^2\left(\frac{\dot{R}}{R}\right)^2 - \frac{5}{12}\left(\frac{\lambda}{mR}\right)^2 - \frac{1}{3}\frac{\ddot{R}}{R}(-3 + \lambda^2), \\ a_{23} &= 0, \quad b_{21} = 2Q - \lambda\frac{m}{R}, \quad b_{22} = 2\frac{\dot{R}}{R}, \quad b_{23} = 0, \\ \\ a_{31} &= 0, \quad a_{32} = 0, \\ a_{33} &= -\frac{1}{3}\dot{\lambda}^2 - \frac{1}{3}\kappa\Lambda - \frac{2}{3}Q^2 - \frac{1}{3}\kappa\rho - \frac{5}{3}\frac{\dot{R}}{R}\lambda\dot{\lambda} - \frac{1}{3}\ddot{\lambda}\lambda \\ &\quad + \frac{2}{3}\frac{m}{R}\lambda Q - \frac{2}{3}\frac{\dot{R}^2}{R^2}\lambda^2 - \frac{1}{6}\lambda^2\frac{m^2}{R^2} - \frac{1}{3}\frac{\ddot{R}}{R}(-3 + \lambda^2), \\ b_{31} &= 0, \quad b_{32} = 0, \quad b_{33} = 2\frac{\dot{R}}{R}, \end{aligned}$$

$$\begin{aligned}
d_1 &= d_3 = 0, \\
d_2 &= R^2[-12\lambda(\frac{\dot{R}}{R})^3 + \lambda\frac{\dot{R}^2}{R^2}(-6 + 13\lambda^2) + 2\dot{\lambda}^3 + \lambda^2(\ddot{\lambda} + \lambda\frac{\ddot{R}}{R}) \\
&\quad + \dot{\lambda}(4Q^2 + \kappa(2\Lambda - \rho) - 6\frac{m}{R}Q\lambda + \lambda(5\ddot{\lambda} + 2\lambda\frac{m^2}{R^2} + 9\lambda\frac{\ddot{R}}{R})) \\
&\quad + \frac{\dot{R}}{R}(\ddot{\lambda}(3 + 7\lambda^2) + \lambda(17\dot{\lambda}^2 + 2\kappa\Lambda - 2Q^2 - \kappa\rho + \frac{m}{R}\lambda Q) \\
&\quad + \lambda\frac{\ddot{R}}{R}(3 + 5\lambda^2))], \\
\text{for } i \neq j &: a_{ij} = -a_{ji}, b_{ij} = -b_{ji}.
\end{aligned}$$

The symmetric parts of Einstein-Cartan equations are given as:

$$\begin{aligned}
(\hat{0}\hat{0}) &: -2\lambda^2\frac{\ddot{R}}{R} + \frac{\dot{R}^2}{R^2}(3 - \lambda^2) + \frac{m^2}{4R^2}(-4 + 3\lambda^2) - 2\frac{\dot{R}}{R}\dot{\lambda} = \kappa(\rho + \Lambda) + \frac{2m\lambda Q}{R} - Q^2, \\
(\hat{1}\hat{1}) &: 2(1 - \lambda^2)\frac{\ddot{R}}{R} + (1 - \lambda^2)\frac{\dot{R}^2}{R^2} - \frac{m^2\lambda^2}{4R^2} - \dot{\lambda}^2 - 5\frac{\dot{R}}{R}\dot{\lambda} - \ddot{\lambda} = \kappa\Lambda + Q^2 - \frac{m\lambda Q}{R}, \\
(\hat{2}\hat{2}) &: 2\frac{\ddot{R}}{R} + (1 - 3\lambda^2)\frac{\dot{R}^2}{R^2} - \frac{m^2\lambda^2}{4R^2} - 2\frac{\dot{R}}{R}\dot{\lambda} = \kappa\Lambda + Q^2 - \frac{m\lambda Q}{R}, \\
(\hat{3}\hat{3}) &: (1 - \lambda^2)(2\frac{\ddot{R}}{R} + \frac{\dot{R}^2}{R^2}) - (4 - \lambda^2)\frac{m^2}{4R^2} - 5\frac{\dot{R}}{R}\dot{\lambda} - \dot{\lambda}^2 - \ddot{\lambda} = \kappa\Lambda + Q^2, \\
(\hat{0}\hat{1}) &: \frac{m\lambda}{R}(\lambda\frac{\dot{R}}{R} + \frac{3}{2}\dot{\lambda}) = \dot{Q}\lambda + 2\dot{\lambda}Q + 3\lambda Q\frac{\dot{R}}{R}, \\
(\hat{0}\hat{2}) &: 2\lambda(\frac{\dot{R}^2}{R^2} - \frac{\ddot{R}}{R}) = 0, \\
(\hat{1}\hat{2}) &: \frac{m}{2R}(\dot{\lambda} + 2\lambda\frac{\dot{R}}{R}) = 0.
\end{aligned}$$

In the limit of small  $\lambda^2 \ll 1$  we combine  $\hat{0}\hat{0}$  and  $\hat{1}\hat{1}$  components to approximate the time gradients of the cosmic scale factor:

$$\begin{aligned}
\frac{\dot{R}^2}{R^2} &= \frac{1}{3}(\kappa(\rho + \Lambda) - Q^2 + \frac{2m\lambda Q}{R} + (\frac{m}{R})^2), \\
\frac{\ddot{R}}{R} &= \frac{1}{2}(\frac{2}{3}\kappa\Lambda - \frac{1}{3}\kappa\rho + \frac{4}{3}Q^2 - \frac{5}{3}\frac{m\lambda Q}{R} - \frac{1}{3}(\frac{m}{R})^2).
\end{aligned} \tag{16}$$

The age of the Universe follows immediately:

$$\begin{aligned}
\tau_U(\text{Gyr}) &= \frac{10}{h} \int_{10^{-3}}^1 \frac{da}{a} [\Omega_\Lambda + \Omega_m a^{-3} - \frac{1}{3}Q^2 + \frac{2}{3}\frac{m\lambda Q}{a} + \frac{m^2}{3a^2}]^{-1/2}, \\
\lambda &= \lambda_0 a^{-1}, Q = Q_0 a^{-3/2}; m, \lambda_0, Q_0 \text{ evaluated in the unit } H_0 = 1.
\end{aligned} \tag{17}$$

Note that even a term linear in torsion  $Q$  is negative because [6]  $m\lambda > 0 (m\lambda < 0)$  implies  $Q < 0 (Q > 0)$ .

The relation (3.31) of Ref. [19], as the equation of motion for the angular momentum of the Zeljdovič model, is no more valid.

Let us finally write the CDM spectrum used in numerical evaluations [8]:

$$P(\vec{k}) = |\delta_{\vec{k}}|^2 = \frac{Ak}{(1 + \beta k + \alpha k^{1.5} + \gamma k^2)^2}, \quad (18)$$

$$\beta = 1.7(\Omega_m h^2)^{-1} Mpc, \quad \alpha = 9.0(\Omega_m h^2)^{-1.5} Mpc^{1.5}, \quad \gamma = 1.0(\Omega_m h^2)^{-2} Mpc^2.$$

## V. APPENDIX B

In this appendix it is pointed out the difference between the standard Ellis-Bruni approach and its corrected version applied in this paper. Their variables are defined as [10]:

$$\bar{\mathcal{D}}_\mu \equiv R(t)\rho^{-1}h_\mu{}^\nu\tilde{\nabla}_\nu\rho, \quad (19)$$

$$\bar{\mathcal{L}}_\mu \equiv R(t)h_\mu{}^\nu\tilde{\nabla}_\nu\Theta.$$

The same procedure as in Appendix A results in the following equation for a density-contrast in the matter dominated epoch:

$$\begin{aligned} & \ddot{\bar{\mathcal{D}}}_\mu + a_\mu a^\lambda \bar{\mathcal{D}}_\lambda + u_\mu \dot{a}^\lambda \bar{\mathcal{D}}_\lambda + u_\mu a^\lambda \dot{\bar{\mathcal{D}}}_\lambda - \frac{1}{2}\kappa\rho\bar{\mathcal{D}}_\mu \\ & + (\dot{\bar{\mathcal{D}}}_\lambda + \bar{\mathcal{D}}_\nu(\sigma^\nu{}_\lambda + \tilde{\omega}^\nu{}_\lambda))\left(\frac{2}{3}\Theta\delta_\mu^\lambda + u_\mu a^\lambda + \tilde{\omega}_{,\mu}^\lambda + \sigma_{,\mu}^\lambda\right) \\ & + \frac{2}{3}\Theta u_\mu a^\nu \bar{\mathcal{D}}_\nu + \dot{\bar{\mathcal{D}}}_\lambda(\tilde{\omega}_{,\mu}^\lambda + \sigma_{,\mu}^\lambda) + \bar{\mathcal{D}}_\lambda(\dot{\sigma}_{,\mu}^\lambda + \dot{\tilde{\omega}}_{,\mu}^\lambda) \\ & - R[2a_\mu\dot{\Theta} + {}^{(3)}\tilde{\nabla}_\mu\mathcal{N} + \Theta a_\lambda\left(\frac{2}{3}\Theta\delta_\mu^\lambda + u_\mu a^\lambda + \tilde{\omega}_{,\mu}^\lambda + \sigma_{,\mu}^\lambda\right) \\ & \quad + \frac{1}{3}\Theta^2 a_\mu + \Theta\dot{a}_\mu] = 0. \end{aligned} \quad (20)$$

The corresponding equations in the local Lorentzian frame are:

$$\ddot{\bar{\mathcal{D}}}_i + \bar{b}_{ij}\dot{\bar{\mathcal{D}}}_j + \bar{a}_{ik}\bar{\mathcal{D}}_k + \bar{d}_i = 0, \quad i, j, k = 1, 2, 3, \quad (21)$$

$$\bar{a}_{11} = 2\frac{\dot{R}^2}{R^2} + \frac{\ddot{R}}{R} - Q^2 - \frac{1}{2}\kappa\rho + \frac{m}{R}\lambda Q - \left(\frac{\lambda m}{2R}\right)^2,$$

$$\bar{a}_{12} = \frac{1}{2}\frac{m}{R}\dot{\lambda} - \frac{7}{4}\frac{\dot{R}}{R}Q + \frac{3}{2}\lambda\frac{m\dot{R}}{R^2}, \quad \bar{a}_{13} = 0,$$

$$\bar{b}_{11} = 4\frac{\dot{R}}{R}, \quad \bar{b}_{12} = -2Q + \lambda\frac{m}{R}, \quad \bar{b}_{13} = 0,$$

$$\bar{a}_{21} = -\frac{1}{2}\dot{\lambda}\frac{m}{R} + \frac{7}{4}\frac{\dot{R}}{R}Q - \frac{3}{2}\lambda\frac{\dot{R}m}{R^2},$$

$$\begin{aligned} \bar{a}_{22} &= \frac{\ddot{R}}{R} - \dot{\lambda}^2 - Q^2 - \frac{1}{2}\kappa\rho - 2\lambda\dot{\lambda}\frac{\dot{R}}{R} \\ &+ \frac{m}{R}Q\lambda - \left(\lambda\frac{m}{2R}\right)^2 - \left(\frac{\dot{R}}{R}\right)^2(-2 + \lambda^2), \end{aligned}$$

$$\bar{a}_{23} = 0, \quad \bar{b}_{21} = 2Q - \lambda\frac{m}{R}, \quad \bar{b}_{22} = 4\frac{\dot{R}}{R}, \quad \bar{b}_{23} = 0,$$

$$\bar{a}_{31} = 0, \quad \bar{a}_{32} = 0, \quad \bar{a}_{33} = 2\frac{\dot{R}^2}{R^2} + \frac{\ddot{R}}{R} - \frac{1}{2}\kappa\rho,$$

$$\bar{b}_{31} = 0, \quad \bar{b}_{32} = 0, \quad \bar{b}_{33} = 4\frac{\dot{R}}{R},$$

$$\bar{d}_1 = \bar{d}_3 = 0,$$

$$\begin{aligned} \bar{d}_2 &= R[2\dot{\lambda}^3 + \lambda^2(\ddot{\lambda} + \frac{\ddot{R}}{R}) + \left(\frac{\dot{R}}{R}\right)^2\dot{\lambda}(6 + 13\lambda^2) \\ &+ \dot{\lambda}(4Q^2 + \kappa(2\Lambda - \rho)) - 6\frac{m}{R}\lambda Q \\ &+ \lambda(5\ddot{\lambda} + 2\lambda\frac{m^2}{R^2} + 9\lambda\frac{\ddot{R}}{R}) \\ &+ \frac{\dot{R}}{R}(\ddot{\lambda}(3 + 7\lambda^2) + \lambda(17\dot{\lambda}^2 + 2\kappa\Lambda - 2Q^2 \\ &- \kappa\rho + \frac{m}{R}\lambda Q + \lambda\frac{\ddot{R}}{R}(3 + 5\lambda^2))], \end{aligned}$$

$$\text{for } i \neq j : \bar{a}_{ij} = -\bar{a}_{ji}, \quad \bar{b}_{ij} = -\bar{b}_{ji}.$$

The authors in [10] equalize components of their variables  $\bar{\mathcal{D}}_\mu$  with a scalar density-contrast  $\delta$ . This is possible in the Friedmann limes when all components are equal. However even then, the scalar quantity formed from their variables must be ad hoc multiplied by the cosmic scale factor to achieve the correct result:

$$\delta \propto R(t)[- \bar{\mathcal{D}}_\mu \bar{\mathcal{D}}^\mu]^{1/2}.$$

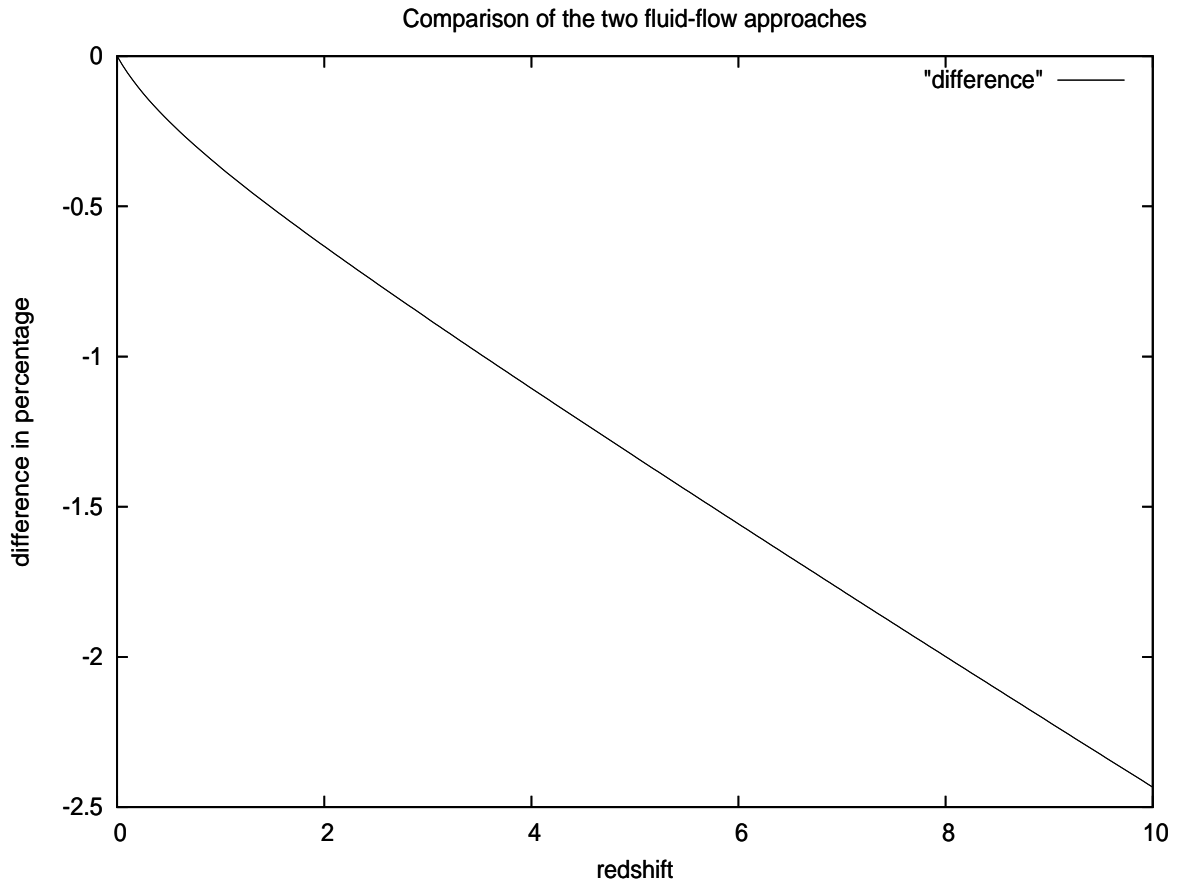


FIG. 4: Comparison between the two fluid-flow approaches for the model EC3:  $\delta \equiv [-\mathcal{D}_\mu \mathcal{D}^\mu]^{1/2}$  and  $\bar{\delta} \equiv R(t)[-\bar{\mathcal{D}}_\mu \bar{\mathcal{D}}^\mu]^{1/2}$ ,  $\text{difference} \equiv (\delta - \bar{\delta})/\delta$ ,  $\delta(z=0) = \bar{\delta}(z=0) = 1$ .

Our corrected variables  $\mathcal{D}_\mu$ , on the contrary, give immediately good and correct Friedmann limes:

$$\delta \propto [-\mathcal{D}_\mu \mathcal{D}^\mu]^{1/2} = [-\mathcal{D}_a \mathcal{D}^a]^{1/2} \quad (22)$$

Let us stress that beyond Friedmannian geometry two quantities are not equal:

$$R(t)[-\bar{\mathcal{D}}_\mu \bar{\mathcal{D}}^\mu]^{1/2} \neq [-\mathcal{D}_\mu \mathcal{D}^\mu]^{1/2},$$

hence we use throughout our paper corrected variables  $\mathcal{D}_\mu$ . In Fig. 4 the reader can find comparison between two formulas when the vorticity and the acceleration do not vanish.

- 
- [1] D. Palle, *Nuovo Cim. A* **109**, 1535 (1996).
- [2] D. Palle, *Nuovo Cim. B* **115**, 445 (2000); D. Palle, *Nuovo Cim. B* **118**, 747 (2003).
- [3] F. Aharonian et al. (H.E.S.S. Collaboration), *Phys. Rev. Lett.* **97**, 221102 (2006).
- [4] D. P. Finkbeiner, *Astrophys. J.* **614**, 186 (2004).
- [5] D. Palle, *Nuovo Cim. B* **111**, 671 (1996).
- [6] D. Palle, arXiv:0802.2060v2 (2008).
- [7] P. J. E. Peebles, *The Large-Scale Structure of the Universe* (Princeton University Press, New Jersey, 1980).
- [8] E. W. Kolb and M. S. Turner, *The Early Universe* (Addison-Wesley, Redwood City, 1990).
- [9] T. Padmanabhan, *Structure formation in the Universe* (Cambridge University Press, Cambridge, 1995).
- [10] G. F. R. Ellis and M. Bruni, *Phys. Rev. D* **40**, 1804 (1989); G. F. R. Ellis, J. Hwang and M. Bruni, *Phys. Rev. D* **40**, 1819 (1989); G. F. R. Ellis, M. Bruni and J. Hwang, *Phys. Rev. D* **42**, 1035 (1990).
- [11] J. M. Stewart and M. Walker, *Proc. R. Soc. Lond. A* **341**, 49 (1974).
- [12] M. J. Longo, arXiv:0812.3437 (2008).
- [13] A. Cooray, *Phys. Rev. D* **65**, 103510 (2002).
- [14] A. Kashlinsky, F. Atrio-Barandela, D. Kocevski and H. Ebeling, *Astrophys. J. Lett.* **686**, L49 (2008).
- [15] R. Watkins, H. A. Feldman and M. J. Hudson, *M.N.R.A.S.* **392**, 743 (2009).
- [16] K. Land and J. Magueijo, *Phys. Rev. Lett.* **95**, 071301 (2005).
- [17] M. R.olta et al. (WMAP Collaboration), arXiv:0803.0593v2 (2008).
- [18] J. A. Schouten, *Ricci-Calculus* (Springer Verlag, Berlin, 1954).
- [19] Yu. N. Obukhov and V. A. Korotky, *Class. Quantum Grav.* **4**, 1633 (1987).
- [20] Th. Chrobok, Yu. N. Obukhov and M. Scherfner, *Phys. Rev. D* **63**, 104014 (2001).
- [21] Th. Chrobok, H. Herrmann and G. Rueckner, *Technische Mechanik* **22**, 1 (2002).
- [22] D. Palle, *Nuovo Cim. B* **114**, 853 (1999).
- [23] S. D. Brechet, M. P. Hobson and A. N. Lasenby, *Class. Quant. Grav.* **24**, 6329 (2007).